H_2 processes with CO_2 mitigation: Thermo-economic modeling and process integration

Laurence Tock[a], François Maréchal[a]

[a]Laboratory for Industrial Energy Systems, Ecole Polytechnique Fédérale de Lausanne
CH – 1015 Lausanne, Switzerland

Submitted to International Journal of Hydrogen Energy (2012)

Abstract

Within the challenge of greenhouse gas reduction, hydrogen is regarded as a promising decarbonized energy vector. The hydrogen production by natural gas reforming and lignocellulosic biomass gasification are systematically analyzed by developing thermo-economic models. Taking into account thermodynamic, economic and environmental factors, process options with CO_2 mitigation are compared and optimized by combining flowsheeting with process integration, economic analysis and life cycle assessment in a multi-objective optimization framework. The systems performance is improved by introducing process integration maximizing the heat recovery and valorizing the waste heat. Energy efficiencies up to 80% and production costs of 12.5-42\$/GJ_{H2} are computed for natural gas H_2 processes compared to 60% and 29-61\$/GJ_{H2} for biomass processes. Compared to processes without CO_2 mitigation, the CO_2 avoidance costs are in the range of 14-306\$/$t_{CO2,avoided}$. The study shows that the thermo-chemical H_2 production has to be analyzed as a polygeneration unit producing hydrogen, captured CO_2, heat and electricity.

*Keywords:*Hydrogen, CO_2 mitigation, Pre-combustion, Polygeneration, Process integration, Thermo-economic optimization

Nomenclature

Abbreviations

ATR Autothermal Reforming
BM Biomass
CC Carbon Capture
CCS Carbon Capture and Storage
CGC Cold Gas Cleaning
E_{imp} Electricity Import
FICFB Fast Internally Circulating Fluidized Bed
GT Gas Turbine
HHV Higher Heating Value
HTS High Temperature Shift
LCA Life Cycle Assessment
LHV Lower Heating Value
LTS Low Temperature Shift
MDEA Methyldiethanolamine
MEA Monoethanolamine
MVR Mechanical Vapor Recompression
NG Natural Gas

NGCC Natural Gas Combined Cycle
POX Partial Oxidation
PSA Pressure Swing Adsorption
Self Self sufficient (in terms of energy)
SMR Steam Methane Reforming
TEA Triethanolamine
WGS Water-Gas Shift

Greek letters

Δh^o Lower heating value, kJ/kg
$\Delta \tilde{h}_r{}^0$ Standard heat of reaction at 25^oC, kJ/mol
ϵ_{eq} Natural gas equivalent efficiency, %
ϵ_{tot} Energy efficiency, %
η_{CO2} CO_2 capture rate, %
θ_{wood} Wood humidity, %wt

Roman letters

C Production cost, \$/GJ
$\dot{E}$ Mechanical/electrical power, kW
$\dot{m}$ Mass flow, kg/s
P Pressure, bar
$\dot{Q}$ Heat, kW
T Temperature, K

Subscripts

cc plant with carbon capture
ref reference plant without carbon capture
res Resource: Natural gas (NG) or wood (BM)

Superscripts

$^+$ Material/energy stream entering the system
$^-$ Material/energy stream leaving the system

1 Introduction

Within the worldwide challenge of global warming mitigation and energy security, renewable resources and carbon capture and storage (CCS) have received considerable attention, especially for hydrogen and electricity production. Biomass-based processes [1] emitting no CO_2 if carefully managed and other renewable H_2 production processes [16] show a high potential towards a sustainable future. H_2 is regarded as a clean, reliable and affordable energy vector that can substitute fossil fuels by the combustion in an internal combustion engine or by electrochemical conversion to electricity in a fuel cell system with high efficiency and without on site CO_2 emissions. In this perspective, the pre-combustion or hydrogen routes are investigated here with regard to different resources (i.e. wood and natural gas) and competing outputs such as H_2 and/or electricity and captured CO_2, and their combination in polygeneration systems.

Several research studies have already identified promising fuel decarbonization processes for H_2 production and/or electricity generation using different resources. As an example some H_2 process performance results are summarized in Table 1. Reported efficiencies range from 69 to 80% for fossil fuel H_2 production [18, 9, 7] and from 51 to 60% for biomass fed processes [14, 29]. In each study, different assumptions are made and different technologies are considered. This yields a large range of performance results making a consistent comparison difficult. The reaction characteristics of H_2 production by reforming and partial oxidation of natural gas have been studied based on thermodynamic analysis in [20, 19, 4] and for biomass processes in [6]. In [2] the economics of producing H_2 from fossil and renewable resources are compared; for natural gas fed processes producing 236-341 t_{H2}/d costs of 19-27\$$_{2007}$/GJ$_{H2}$ with a gas price

of 10.3\$/GJ$_{NG}$ are reported. While for renewable processes using biomass, solar or wind to produce between 1.3 and 354 t$_{H2}$/d costs in the range of 19.5-70.3\$/GJ$_{H2}$ are reported [2]. These costs values are however highly dependent on the resource prices that constitute about one to two third of the cost. These studies [9, 2] comparing H_2 processes using various resources and technologies are mainly based on a literature survey with regard to the production cost and do not include process modeling and optimization.

The co-production of electricity and H_2 from natural gas resources is studied in [7] computing energy and exergy efficiencies to assess the benefit in terms of primary energy consumption and/or reduced CO_2 emissions. Besides performance estimates and thermodynamic arguments, no economic analysis is however performed. In [26] the thermodynamic and engineering aspects of pre-combustion natural gas power plants are studied without including energy integration and economic aspects. However, in [3] it is shown how heat recovery for reactants preheating can increase the H_2 yield by 10%. Whereas for coal based H_2 and electricity co-production processes, the studies in [5, 17] included efficiency and cost evaluations and [8] applied process integration to maximize the overall plant energy efficiency.

To overcome the difficulties of comparing processes with different assumptions, our goal is to propose a comprehensive comparison framework combining thermo-economic models, energy integration techniques and economic evaluation simultaneously. The objective is to compare and optimize fuel decarbonization (pre-combustion) process configurations with regard to energy, economic and environmental considerations by applying a consistent methodology. Special interest is given to the effect of polygeneration of H_2 fuel, captured CO_2, heat and power, in order to identify its advantages and constraints, and to better understand trade-offs between efficiency, investment and emissions.

2 Methodology

The process is divided into a set of process operations that can be realized by different technology options that are considered in a superstructure model presented in Figure 1. After the assessment of candidate process technologies in the superstructure, thermo-economic models are developed following the methodology described in [11] for the conceptual process design assessing systematically the energetic, economic and environmental performance. Figure 2 illustrates the methodology and the interactions between the different models. The chemical and physical transformations and the associated heat transfer requirements are computed in the energy-flow model established with conventional flowsheeting software. The energy-integration model optimizes the heat recovery and the combined fuel, heat and power production by using the heat cascade constraints and a linear programming model minimizing the operating cost [21]. Applying pinch analysis, the optimal process integration is computed and the process needs are satisfied by different utilities including waste and process gas combustion, Rankine cycle, gas turbine and cogeneration. After equipment sizing, the costs are evaluated using the approach and correlations reported in [30, 31]. To evaluate the environmental impact of the process the local CO_2 emissions are considered here, knowing that in a subsequent study the whole life cycle impacts could be assessed following the approach described in [13]. Finally, multi-objective optimization applying an evolutionary algorithm [24] is performed to assess the trade-offs between competing objectives and to identify competitive configurations yielding a good compromise between the different targets.

3 Process Description

The general superstructure presented in Figure 1 summarizes the different technological options that are considered for pre-combustion process designs. The main process steps are resource extraction and treatment, syngas (i.e. H_2 and CO) generation by natural gas (NG) reforming

or biomass (BM) (i.e. wood) gasification, gas cleaning and treatment, H_2 purification and/or H_2 burning for electricity generation. In both natural gas and biomass based H_2 pathways, a CO_2 removal step is included during the H_2 purification which allows for CO_2 capture (CC) and further sequestration for greenhouse gas mitigation. The energy demand of the process can be satisfied by importing electricity or by burning part of the H_2-fuel in a gas turbine (GT) to close the balance. Consequently, depending on the production purpose, the process can produce either H_2 with and without captured CO_2, imports electricity or is self-sufficient in terms of power, or exports electricity if all the H_2-fuel is burnt. When CO_2 is captured, it is pressurized to 110bar to reach the conditions for sequestration. The natural gas fed process layout is illustrated in Figure 3, while Figure 4 represents the biomass conversion process.

3.1 H_2 production from natural gas

Presently, H_2 is essentially produced from natural gas by endothermic steam methane reforming (SMR) (Eq.1) requiring heat supply or by autothermal reforming (ATR) satisfying the SMR heat demand by partial oxidation (POX) (Eq.2) of the fuel with air or pure O_2. Figure 3 presents the process blockflow diagram and Tables 2&3 summarize the modeling assumptions and nominal operating conditions considered in this study. The process models are established with flowsheeting software using literature data [18, 9, 7, 26, 22]. The reforming reactor is modeled as an isothermal reactor following the approach described in [22]. It is assumed that the reactions (Eqs.1&3) reach thermodynamical equilibrium defined by the reaction temperature. The POX reaction (Eq.2) using air as an oxidant is modeled as conversion reaction by imposing complete consumption of the oxygen.

After the reformer, the syngas (H_2-CO mixture) is cooled down for heat recovery purposes and catalytically reacted with H_2O in a water gas shift (WGS) reactor (Eq.3) to increase the H_2 and CO_2 content. A dual shift reactor performing the shift in a successive high temperature (HTS) (i.e. T=623-693K) and low temperature (LTS) (i.e. T=473-523K) reactor is applied to profit from the high temperatures [18]. The WGS reactor is modeled as isothermal reactor and it is assumed that the WGS reaction Eq.3 reaches thermodynamical equilibrium at the specified reaction temperature. The isothermal modeling of the reactor follows the approach outlined in [22] applying the minimum exergy losses representation. This modeling approach allows to decouple the heat transfer from the chemical reaction heat and consequently to maximize the energy recovery for power generation.

$$CH_4 + H_2O \leftrightarrow CO + 3H_2 \quad \Delta\tilde{h}_r^o = 206kJ/mol \tag{1}$$

$$CH_4 + \frac{1}{2}O_2 \leftrightarrow CO + 2H_2 \quad \Delta\tilde{h}_r^o = -36kJ/mol \tag{2}$$

$$CO + H_2O \leftrightarrow CO_2 + H_2 \quad \Delta\tilde{h}_r^o = -41kJ/mol \tag{3}$$

After the shift section, the H_2/CO_2 mixture is separated. First water is removed by condensation to avoid a decrease of the separation efficiency due to high water contents. To generate high purity H_2 and CO_2 simultaneously, chemical absorption with amines (MEA, MDEA, TEA) is followed by a pressure swing absorption step (PSA). The chemical absorption consumes a considerable amount of energy for the solvent regeneration, the flue gas compression and the solvent circulation. In our approach, the removal plant is modeled as a blackbox using the average data in Table 2. This simplified model does not represent the influence of decision variables inside the CO_2 removal process that could allow to increase the CO_2 capture efficiency. This influence is investigated in a another study [28]. Comparing the blackbox model with the detailed model using TEA as a solvent, yields a variation of the heat requirement around 15%. The assessed values are in the range of 3-5GJ/t_{CO2} given in [25]. Taking into account the temperature levels, the difference expressed in terms of exergy is around 90MJ/t_{CO2} (8.5%). This

difference translates in a small efficiency increase of around 1.5%, a variation of the investment cost of a few percent and a production cost variation of 3%. For the PSA model, the approach outlined in [12] is adapted for H_2/CO_2 separation based on data from [15]. The purity and the amount of H_2 and CO_2 recovered in the respective outlet streams is essentially defined by the PSA cycle design, namely the durations of the adsorption, recycling and purging periods. After the CO_2 capture unit the H_2-rich gas exits at the process pressure and after PSA at atmospheric conditions or lower. No H_2 compression for storage and transportation has been included in this study. If CO_2 sequestration is considered, CO_2 compression up to 110bar is included. It has to be noted that the CO_2 purification step possibly required before the CO_2 compression to reach the purity characteristics for transportation and storage (min 95%vol) has been neglected.

The H_2-rich fuel can be used as fuel in boilers, furnaces, gas turbines and fuel cells for power and/or heat generation or as chemical for other applications (Figure 3). Instead of H_2 purification by PSA for H_2 generation, the option of generating electricity by burning the H_2-rich fuel after CO_2 separation is considered. Even if in practice there are still some concerns with regard to backpropagation which have to be addressed for high purity H_2 combustion, it is assumed here that technology developments will make it feasible in the future.

3.2 H_2 production from biomass

The H_2 production by lignocellulosic biomass conversion (Figure 4) consists of wood handling, air drying, indirectly heated fluidized bed gasification (FICFB), cold gas cleaning (CGC) and conditioning by reforming and shift conversion, and finally H_2 purification. The main parameters and operating conditions are summarized in Tables 2&3. After the syngas production, the process steps are identical to the one described for the natural gas process. The biomass fed H_2 process has been studied in detail in a previous study [27] highlighting in particular, how appropriate energy integration and operating conditions optimization improve the process performance by maximizing the combined production of fuel, heat and power.

4 Process Performance

4.1 Performance indicators

The process performance depends on the one hand on the efficiency of the chemical conversion into fuel defined by the technology choice, the operating conditions, the stoichiometry and the product type, and on the other hand on the quality of the process integration that depends on the energy conversion technologies, the heat recovery and the combined heat and power production. The first law energy efficiency ϵ_{tot} is calculated by Eq.4. It takes into account the energy of the products and resources, and considers thermal and mechanical energy as being equivalent. In order to take into account the difference of the quality of the energy, the natural gas equivalent efficiency ϵ_{eq} is defined by Eq.5. In this definition, the consumed electricity is presented by the net electricity output ($\Delta\dot{E}^- = \dot{E}^- - \dot{E}^+$). The net electricity output is substituted by an equivalent amount of natural gas required for generating the same amount of electricity in a combined cycle with an energy efficiency η of 57.3%. The reported efficiencies are expressed on the basis of the lower heating value (Δh^0, LHV).

$$\epsilon_{tot} = \frac{\Delta h^0_{H2,out} \cdot \dot{m}_{H2,out} + \dot{E}^-}{\Delta h^0_{feed,in} \cdot \dot{m}_{feed,in} + \dot{E}^+} \tag{4}$$

$$\epsilon_{eq} = \frac{\Delta h^0_{H2,out} \cdot \dot{m}_{H2,out} + \frac{1}{\eta}\Delta\dot{E}^-}{\Delta h^0_{feed,in} \cdot \dot{m}_{feed,in}} \tag{5}$$

To assess the CO_2 mitigation potential, the CO_2 capture rate is defined (Eq.6) by the ratio between the CO_2 captured and the carbon entering the system. For electricity import, green electricity is considered and consequently no carbon emissions have been accounted for. The CO_2 capture cost is calculated as the CO_2 avoidance cost (Eq.7). It is expressed by the difference of the emissions and the difference of the total cost with regard to a reference plant without CO_2 capture. The reference plant without CO_2 capture produces H_2 ($1530MW_{H2}$) from natural gas with a cost of $7.8\$/GJ_{H2}$ (with $5\$/GJ_{NG}$) and emissions of $137kg_{CO2,emitted}/GJ_{H2}$ using the data from [23]. For the power plant without CO_2 capture the natural gas combined cycle (NGCC) plant ($528MW_e$) with $21.3\$/GJ_e$ (with $9.7\$/GJ_e$) and $102.7kg_{CO2,emitted}/GJ_e$ from [10] is considered.

$$\eta_{CO2} = \frac{molC_{captured}}{molC_{in}} \cdot 100 \tag{6}$$

$$\$/t_{CO2,avoided} = \frac{C_{CC} - C_{ref}}{CO_{2,emit_{ref}} - CO_{2,emit_{CC}}} \frac{[\$/GJ]}{[t_{CO2}/GJ]} \tag{7}$$

The economic performance is evaluated by the capital investment and the production cost using the economic assumptions given in Table 4. The investment is based on the size and the type of construction material of each equipment and is estimated by applying the capacity-based correlations given in [30, 31]. The sizing and cost estimation of the catalytic reforming and shift reactors are based on the data reported in [22]. Whereas, the dimensions and cost of the biomass dryers, the gasifiers and the gas cleaning units are estimated using the data reported in [12].

The different scenarios that are investigated for H_2 and/or electricity generation are:

- biomass gasification (BM)
- natural gas reforming by SMR
- natural gas reforming by ATR

For H_2 generation processes, the possibility to import electricity (E_{imp}) or to burn part of the H_2-rich gas to satisfy the process power demands (self-sufficient, $self$) is considered. The H_2 production is compared with the production of electricity burning the H_2 in a gas turbine (GT) after capturing the CO_2. All scenarios integrate a combined steam cycle. For the configurations using biomass, the performance results reported in [27] have been reevaluated with the base case economic assumptions given in Table 4. The performance analyses are performed for a plant capacity of $725MW_{th,NG}$ of natural gas and $380MW_{th,BM}$ of dry biomass, respectively.

4.2 Multi-objective optimization

The trade-off of competing factors defining the process performance is assessed by multi-objective optimization applying an evolutionary algorithm. The key process operating conditions given in Table 3 are chosen as decision variables. The objectives are the maximization of the overall energy efficiency ϵ_{tot} (Eq.4) and the maximization of the carbon capture rate η_{CO2} (Eq.6). The optimal Pareto frontiers for the different H_2 processes are presented in Figure 5. They show that CO_2 capture reduces the efficiency due to the energy consumption for CO_2 separation and compression. Figure 6 shows for the natural gas processes the trade-off between efficiency, CO_2 capture and production cost. High efficiency processes have lower production cost due to the higher H_2 production but also higher CO_2 emissions. While high CO_2 capture rates reduce the efficiency and increase the production cost due to the additional investment and the increase of the energy demand for CO_2 capture. For each scenario one configuration yielding a compromise between efficiency and CO_2 capture is chosen in order to compare in detail the performances of the different process configurations. For natural gas processes the Pareto optimal configuration

corresponding to a capture rate of 90% is chosen, while for biomass conversion processes the one with 65% capture rate is selected. For biomass conversion a lower capture rate can be considered in order to reach a higher efficiency ϵ_{tot}, because it corresponds to the capture of biogenic CO_2. CO_2 capture generates in this case a negative balance since the captured carbon comes from the CO_2 assimilated in the biomass by photosynthesis. The specific performance results of the selected configurations are summarized in Table 5. For the H_2 processes the performances are expessed per GJ of H_2 produced based on the lower heating value, while for the processes generating only electricity they are expressed per GJ of electricity produced.

4.3 Performance comparison: H_2 production

The comparison of the H_2 processes using different resources and importing electricity (E_{imp}) or being self-sufficient (self) in terms of power shows that the highest efficiency is reached for natural gas SMR processes importing electricity (Figure 5). The performances are analyzed and discussed in detail in the following sections.

4.3.1 Energy integration

For self-sufficient H_2 processes, the composite curves presented in Figure 7 reveal the difference in the energy demands. The endothermic gasification and SMR processes require heat supply for the syngas generation, while in the ATR process the heat is delivered internally by a POX reaction. As a consequence, the ATR process requires the lowest hot utility. The heat demands above the pinch point are satisfied by the combustion of off-gases and, if necessary, of part of the H_2-rich gas. In the purification step, the CO_2 separation by chemical absorption requires a large amount of energy for the amine-solvent regeneration. Below the pinch point, the heat excess is valorized in a steam network for electricity generation. In these configurations, the quality of the energy integration is improved by introducing a mechanical vapor recompression (MVR) between the absorber (condensation at 429K) and the stripper (evaporation at 378K). Although it is realized below the pinch point, the MVR integration appears to be energetically needed because the combined production of heat and power creates a utility pinch point at the level of the desorption. Introducing the MVR, reduces the medium pressure steam usage needed for the CO_2 desorber. This steam can be expanded to very low pressure in the condensing turbine stage which maximizes the combined production of power. The increase of mechanical power production is larger than the amount required to compensate the mechanical power needed by the compression in the MVR. Through the conversion of waste heat into mechanical power the efficiency is increased by 3%-points (Table 5). Even if the productivity is increased, the production cost remain nearly constant due to the increased capital cost for the compressor purchase.

4.3.2 Power balance

The variation of the efficiency reflects the difference in the power demand and supply (Table 5). The power balance reported in Figure 8 shows that the largest power demand is attributed to gas treatment and purification including CO_2 separation and CO_2 compression. Moreover, the heat pumping improving the capture unit integration requires power for the compression. Power is generated by the steam network and the gas turbine burning off-gases. For self-sufficient configurations, the balance is closed by burning part of the H_2 product in a gas turbine, while for the other scenarios electricity is imported from the grid.

For the ATR processes, using air as oxidant, some N_2 remains in the products yielding a H_2 purity around 96%mol compared to over 99.5%mol for SMR and BM processes. The purification of the syngas produced by ATR is more power demanding and more expensive due to the larger flows to be treated. In addition, air has to be compressed to the operating pressure explaining the larger power demand for the synthesis. Feeding the ATR with pure O_2 might become an

alternative if one wants to reach purities over 99%mol H_2. Adding pure O_2 has the advantage that no N_2 is present in the downstream process which reduces the equipment size and facilitates CO_2 capture, however it requires pure O_2 to be produced in an air separation unit. This trade-off remains to be investigated in future studies.

Comparing the self-sufficient H_2 processes, the SMR process has the lowest power consumption (Figure 8) explaining the higher efficiency (ϵ_{tot}=78%) even if the thermal energy demand is larger (Figure 7). The power demand is reduced by 18% and 34% when compared with the ATR and the BM process respectively. Since less process gas has to be burnt in a gas turbine for power generation more H_2 is produced. The H_2 productivity is decreased by 6% for the ATR and by 45% for the BM process. The lower efficiency of the biomass process is related to the lower energy content compared to the natural gas resource. These trends are also reflected by the difference in the production costs reported in Figure 9.

With electricity import, the energy efficiency (ϵ_{tot}) of the ATR process is increased by nearly 5%-points and of the biomass by more than 16%-points because more H_2 is produced since none has to be burnt for power generation. However, expressed in terms of natural gas equivalent efficiency Eq.5, the efficiency of the self-sufficient scenario is nearly 3%-points higher for the ATR process and over 6%-points for the BM process. This shows that the internal electricity generation is more efficient than the separate production of electricity from natural gas. The marginal production expressed by $\Delta\dot{E}/\Delta H_2$ is around 70% for the ATR and biomass processes. Even if, 13% more H_2 is produced for the ATR process, Figure 9 shows that the production costs are around 15% higher due to the electricity purchase at the price of green electricity (75\$/GJ_e). An electricity purchase price of around 34.7\$/GJ_e makes the two solutions equivalent.

4.3.3 Economic performance

The economic performance expressed in terms of production cost in Figure 9 is related to the productivity. The natural gas processes have lower production costs due to the higher H_2 yield. The production costs are composed mainly of the resource purchase, the annual investment and electricity purchase for configurations with electricity import. The production costs of the biomass gasification processes are high because of the lower efficiency and the larger investment required especially for the gasifier purchase that corresponds to about 1/3 of the capital costs. It is to note that the equipment sizing and costing method might overestimate the equipment costs; nevertheless biomass gasification being an emerging technology is more expensive than the well established reforming technologies.

Resource price influence The influence of the resource price on the economic performance is illustrated in Figure 10. The natural gas and biomass price are varied between the low and high economic assumptions as given in Table 4. The assessed production costs in the range of 12.5-61\$/GJ_{H2} are comparable to the one reported in [2] for fossil and renewable resources and competitive with the costs of 7.5-14\$/GJ_{H2} assessed in the IPCC report [23] for a H_2 plant with CO_2 capture using natural gas. The reference processes published in [23] feature lower efficiency and are therefore considered as suboptimal. Through good process integration over 15% higher efficiencies are reached in this study. Biomass gasification technology development could lead to a capital cost reduction and consequently to more competitive biomass processes in the future.

CO_2 avoidance cost The CO_2 mitigation potential is assessed by the CO_2 avoidance costs reported in Figure 11 taking into account the influence of the resource prices (Table 4) on the production cost. Considering as a reference a H_2 plant without CO_2 capture from [23], the computed costs (36-263\$/$t_{CO2,avoided}$) are comparable to the ones reported in [23] (2-56\$/$t_{CO2,avoided}$) with a resource price around 5\$/GJ_e. With CO_2 mitigation, CO_2 emissions in H_2 plants using natural gas can be reduced to around 7.5$kg_{CO2,emitted}$/GJ_{H2}, while for the biomass process the

CO_2 emissions are biogenic and consequently accounted as being null or even negative if CO_2 is captured.

These results reveal that fuel decarbonization for H_2 production is not only competitive with regard to environmental considerations but also with regard to energetic and economic performance for specific resource prices and CO_2 taxes.

4.4 Performance comparison: Electricity generation

Instead of generating pure H_2 the option to generate electricity by burning the H_2-fuel in a gas turbine after CO_2 capture is investigated. The performance results of the different scenarios are compared in Figure 12 and Table 5. Compared to a conventional NGCC plant without CO_2 capture generating electricity with an efficiency of 55-58%, production costs of 18-24\$/GJ_e and CO_2 emissions of 100-105$kg_{CO2,emitted}/GJ_e$ [10], CO_2 mitigation reduces the efficiency by around 8%-points and increases the costs by around 20% due to the energy demand and costs of CO_2 capture by chemical absorption and CO_2 compression. With pre-combustion CO_2 capture, production costs in the range of 22.7-50\$/GJ_e are assessed for natural gas based processes with an efficiency of around 55% compared to 28% and 46.6-96\$/GJ_e for biomass fed processes taking into account the resource price variation [5.5-19.5\$/GJ_{res}]. With CO_2 avoidance costs of 14-306\$/$t_{CO2,avoided}$ and 72-212\$/$t_{CO2,avoided}$ for natural gas and biomass processes respectively, CO_2 capture is promising with regard to future energy market, especially when high CO_2 taxes are imposed. The use of biomass become competitive compared to fossil resources with regard to environmental considerations and even from an economical point of view if technology cost can be reduced. The analyzed pre-combustion processes reveal to be competitive compared to an NGCC power plant with post-combustion CO_2 capture yielding an efficiency of about 50%, production costs in the range of 23-35\$/GJ_e (with 9.7\$/GJ_{NG}) and CO_2 avoidance cost around 62-128\$/$t_{CO2,avoided}$ [10]. Depending on the production purpose and the market scope, the decision between generating electricity or H_2 with electricity import or self-sufficient, with or without CO_2 mitigation can be made with the proposed model.

5 Conclusions

The competitiveness of the H_2 production and/or electricity generation from natural gas and biomass resources with CO_2 mitigation is compared with regard to energy efficiency, cost and environmental impacts based on thermo-economic models. Process integration techniques and multi-objective optimizations are applied to assess the trade-offs and to reveal the potential of polygeneration of H_2, heat and power, and captured CO_2. Under selected economic assumptions, CO_2 avoidance costs in the range of 36-263\$/$t_{CO2,avoided}$ are obtained for H_2 plants and 14-306\$/$t_{CO2,avoided}$ for power generation. Natural gas and biomass resources are compared and the sensitivity to their prices are analyzed. For biomass based processes the cost of the gasifier is critical since it accounts for more than one third of the production cost at low resource prices. It is shown that the competitiveness highly depends on the resource price, the imposed CO_2 taxes and the production scope. With regard to climate change mitigation, fuel decarbonization for H_2 and/or electricity generation using fossil and even renewable resources reveal to be competitive solutions when compared with oxy-fuel and post-combustion CO_2 capture.

Acknowledgement

This work was done in the frame of the CARMA project "Carbon Dioxide Management in Power Generation" funded by the Competence Center Environment and Sustainability (CCES) and the Competence Center Energy and Mobility (CCEM) of the Swiss ETH domain.

References

[1] H. Balat and E. Kirtay. Hydrogen from biomass - present scenario and future prospects. *International Journal of Hydrogen Energy*, 35(14):7416–7426, July 2010.

[2] J. R. Bartels, M. B. Pate, and N. K. Olson. An economic survey of hydrogen production from conventional and alternative energy sources. *International Journal of Hydrogen Energy*, 35(16):8371–8384, Aug. 2010.

[3] W. Chen, T. Chiu, and C. Hung. Enhancement effect of heat recovery on hydrogen production from catalytic partial oxidation of methane. *International Journal of Hydrogen Energy*, 35(14):7427–7440, July 2010.

[4] W. Chen, M. Lin, J. Lu, Y. Chao, and T. Leu. Thermodynamic analysis of hydrogen production from methane via autothermal reforming and partial oxidation followed by water gas shift reaction. *International Journal of Hydrogen Energy*, 35(21):11787–11797, Nov. 2010.

[5] P. Chiesa, S. Consonni, T. Kreutz, and R. Williams. Co-production of hydrogen, electricity and CO2 from coal with commercially ready technology. part a: Performance and emissions. *International Journal of Hydrogen Energy*, 30(7):747–767, 2005.

[6] M. Cohce, I. Dincer, and M. Rosen. Thermodynamic analysis of hydrogen production from biomass gasification. *International Journal of Hydrogen Energy*, 35(10):4970–4980, May 2010.

[7] S. Consonni and F. Viganò. Decarbonized hydrogen and electricity from natural gas. *International Journal of Hydrogen Energy*, 30(7):701–718, 2005.

[8] C. Cormos. Evaluation of energy integration aspects for IGCC-based hydrogen and electricity co-production with carbon capture and storage. *International Journal of Hydrogen Energy*, 35(14):7485–7497, July 2010.

[9] K. Damen, M. v. Troost, A. Faaij, and W. Turkenburg. A comparison of electricity and hydrogen production systems with CO2 capture and storage. part a: Review and selection of promising conversion and capture technologies. *Progress in Energy and Combustion Science*, 32(2):215–246, 2006.

[10] M. Finkenrath. Cost and performance of carbon dioxide capture from power generation. Technical report, International Energy Agency, 2011.

[11] M. Gassner and F. Maréchal. Methodology for the optimal thermo-economic, multi-objective design of thermochemical fuel production from biomass. *Computers & Chemical Engineering*, 33(3):769–781, 2009.

[12] M. Gassner and F. Maréchal. Thermo-economic process model for the thermochemical production of Synthetic Natural Gas (SNG) from lignocellulosic biomass. *Biomass & Bioenergy*, 33(11):1587–1604, 2009.

[13] L. Gerber, M. Gassner, and F. Maréchal. Systematic integration of LCA in process systems design: Application to combined fuel and electricity production from lignocellulosic biomass. *Computers & Chemical Engineering*, 35(7):1265 – 1280, 2011.

[14] C. N. Hamelinck and A. P. C. Faaij. Future prospects for production of methanol and hydrogen from biomass. *Journal of Power Sources*, 111(1):1–22, 2002.

[15] J. Jee, M. Kim, and C. Lee. Adsorption characteristics of hydrogen mixtures in a layered bed: Binary, ternary, and Five-Component mixtures. *Industrial & Engineering Chemistry Research*, 40(3):868–878, 2001.

[16] C. Koroneos, A. Dompros, G. Roumbas, and N. Moussiopoulos. Life cycle assessment of hydrogen fuel production processes. *International Journal of Hydrogen Energy*, 29(14):1443–1450, Nov. 2004.

[17] T. Kreutz, R. Williams, S. Consonni, and P. Chiesa. Co-production of hydrogen, electricity and CO2 from coal with commercially ready technology. part b: Economic analysis. *International Journal of Hydrogen Energy*, 30(7):769–784, 2005.

[18] J. Longanbach, M. Rutkowski, M. Klett, J. White, R. Schoff, and T. Buchanan. Hydrogen production facilities plant performance and cost comparisons. Technical report, Report prepared for the USDOE National Energy Technology Laboratory (NETL) by Parsons Infrastructure and Technology Group, Inc., 2002.

[19] A. E. Lutz, R. W. Bradshaw, L. Bromberg, and A. Rabinovich. Thermodynamic analysis of hydrogen production by partial oxidation reforming. *International Journal of Hydrogen Energy*, 29(8):809–816, 2004.

[20] A. E. Lutz, R. W. Bradshaw, J. O. Keller, and D. E. Witmer. Thermodynamic analysis of hydrogen production by steam reforming. *International Journal of Hydrogen Energy*, 28(2):159–167, 2003.

[21] F. Maréchal and B. Kalitventzeff. Process integration: Selection of the optimal utility system. *Computers & Chemical Engineering*, 22:149–156, 1998.

[22] F. Marechal, F. Palazzi, J. Godat, and D. Favrat. Thermo-Economic modelling and optimisation of fuel cell systems. *Fuel Cells*, 5(1):5–24, 2005.

[23] B. Metz, O. Davidson, H. de Coninck, M. Loos, and L. Meyer. IPCC special report on carbon dioxide capture and storage. Technical report, Cambridge University Press, 2005.

[24] A. Molyneaux, G. Leyland, and D. Favrat. Environomic multi-objective optimisation of a district heating network considering centralized and decentralized heat pumps. *Energy*, 35(2):751–758, 2010.

[25] P. Radgen, C. Cremer, S. Warkentin, P. Gerling, F. May, and S. Knopf. Verfahren zur CO2-Abscheidung und -Speicherung. Abschlussbericht Forschungsbericht 20341110 UBA-FB 000938, Frauenhofer-Institut für Systemtechnik und Innovationsforschung, Bundesantstalt für Geowissenschaften und Rohstoffe, 2005.

[26] M. C. Romano, P. Chiesa, and G. Lozza. Pre-combustion CO2 capture from natural gas power plants, with ATR and MDEA processes. *International Journal of Greenhouse Gas Control*, 4(5):785–797, Sept. 2010.

[27] L. Tock and F. Maréchal. Co-production of Hydrogen and Electricity from Lignocellulosic Biomass: Process Design and Thermo-economic Optimization. *Energy*, 2012.

[28] L. Tock and F. Maréchal. Thermo-chemical hydrogen production process design, optimization and comparison based on life cycle assessment. World Hydrogen Energy Conference, Toronto, Canada, 2012.

[29] R. Toonssen, N. Woudstra, and A. Verkooijen. Exergy analysis of hydrogen production plants based on biomass gasification. *International Journal of Hydrogen Energy*, 33(15):4074–4082, 2008.

[30] R. Turton. *Analysis, Synthesis, and Design of Chemical Processes*. Prentice Hall, Upper Saddle River, N.J, 3rd ed edition, 2009.

[31] G. Ulrich and P. Vasudevan. *A Guide to Chemical Engineering Process Design and Economics a Practical Guide*. CRC, Boca Raton, Fla, 2nd ed edition, 2003.

List of Tables

Table 1: Reference H_2 production plants performance.

Process	CO_2 capt. [%]	ϵ [%]	[\$/GJ$_{H2}$]	[t$_{H2}$/d]	Res. price	Ref.
Natural gas	0	83.9 (HHV)	5.2	418	3\$/GJ$_{NG}$	[18]
Natural gas	71	78.6 (HHV)	5.6	418	3\$/GJ$_{NG}$	[18]
Coal (Texaco gasif.)	0	63.7 (HHV)	8.7	309	29\$/t	[2]
Coal (Texaco gasif.)	87	59 (HHV)	10.5	281	29\$/t	[2]
Biomass (FICFB, CGC)	-	57.7	-	-	-	[29]
Biomass	-	51-60	8-11	90-184	2\$/GJ$_{BM}$	[14]

Table 2: Parameters for the energy-flow models.

Section	Specification	Value
Biomass feedstock	Composition [%wt]	C=51.09%, H=5.75%
		O=42.97%, N=0.19%
	$\theta_{wood,in}$	50%wt
Natural gas feedstock	Composition	CH_4= 100 %
Chemical absorption	$\dot{Q}$ @ 423K	3.7MJ$\cdot kg^{-1}$ CO_2
(95% efficiency) [25]	Electric Power	1.0MJ$\cdot kg^{-1}$ CO_2
Physical adsorption	Adsorption P	10bar
	Purging P	0.1bar
	H_2 recovery	90%
CO_2 compression	P	110bar
	$\eta_{compressor}$	85%
Gas turbine	$\eta_{compressor}$	85%
	$\eta_{turbine}$	90%

Table 3: Operating conditions of the process units and feasible range for optimization.

Section	Specification	Nominal	Range
Biomass drying	T [K]	473	-
Biomass pyrolysis	T [K]	533	-
Biomass gasification	$\theta_{wood,gasif\_in}$ [%wt]	20	[5-35]
	T [K]	1123	[1000-1200]
	P [bar]	1	[1-15]
	Steam/biomass [%wt]	50	-
SMR after gasification	T [K]	1138	[950-1200]
SMR	T [K]	1073	[725-1200]
	P [bar]	11	[1-30]
	S/C [-]	3	[1-6]
ATR	T [K]	1173	[780-1400]
	P [bar]	15	[1-30]
	S/C [-]	2.5	[0.5- 6]
WGS	T$_{HTS}$ (NG/BM) [K]	633/623	[523-683]/[573-683]
	T$_{LTS}$ (NG/BM) [K]	473/453	[423-523]/[423-573]
	P (BM) [bar]	25	[1-25]
	S/C (BM) [-]	2	[0.2-4]
Gas turbine	Combustion inlet T [K]	773	-
	Turbine inlet T [K]	1680	-

Table 4: Assumptions for the economic analysis.

Scenario	low	base	high
Marshall and Swift Index [-]		1473.3	
Dollar exchange rate [US$/€]		1.2	
Expected lifetime [years]		25	
Interest rate [%]		6	
Yearly operation [h/year]		7500	
Wood costs (θ_{wood}=50% wt) [$ /GJ$_{BM}$]	5.5	13.9	19.5
Natural gas costs [$ /GJ$_{NG}$]	5.5	9.7	19.5
Electricity import price (green) [$ /GJ$_e$]	41.7	75	83.4

Table 5: Investigated process configurations performances considering the economic assumptions given in Table 4. For H_2 processes the specific performances are expressed per GJ$_{H2}$, while for electricity generation processes they are expressed per GJ$_e$. The net electricity output expressed in MJ of electricity per GJ of hydrogen or electricity produced is negative when the integrated process requires electricity importation and positive when it generates electricity.

	H_2 Process							Electricity generation		
Process Parameters										
Products	H_2	H_2	H_2	H_2	H_2	H_2	H_2	$\dot{E}$	$\dot{E}$	$\dot{E}$
Process	ATR self	ATR self no MVR	SMR self	BM self	ATR E$_{imp}$	SMR E$_{imp}$	BM E$_{imp}$	ATR GT	SMR GT	BM GT
Installation MWth$_{NG/BM}$	725	725	725	380	725	725	380	725	725	380
CO_2 capture [%]	89.9	89.9	88.5	64.3	89.6	89.3	65	89.2	90	65.6
Power Balance										
Consumption [MJ/GJ]	240.3	206	184.3	508.3	221.6	172.4	291.2	152.3	125.2	643.9
Steam network [MJ/GJ]	69.1	52.2	44.3	155.4	55.4	0	8.1	151.7	131.3	524.7
Gas turbine [MJ/GJ]	171.2	153.8	140	352.9	71.1	25.7	17.9	1000.6	993.9	1119.2
Net electricity [MJ/GJ]	0	0	0	0	-95.1	-146.7	-265.2	1000	1000	1000
Performance										
Product [MJ/GJ$_{res}$]	732.8	703.2	784.2	432.5	844.6	937.2	724.2	544.4	564.3	281.1
H_2 purity [mol%]	96.3	96.3	99.8	99.5	96.3	99.9	99.6	(65)	(98.2)	(89.5)
H_2 production [t/d]	382.5	367.1	409.3	118.3	440.9	489.2	198.1	-	-	-
kg$CO_{2,emitted}$/GJ	7.5	7.9	8.1	-149	6.7	6.3	-90	11	9.8	-294
ϵ_{tot} [%]	73.3	70.3	78.4	43.2	78.2	82.4	60.1	54.4	56.4	28.1
ϵ_{eq} [%]	73.3	70.3	78.4	43.2	70.4	69.7	36.6	-	-	-
Economics										
Investment [$/kW$_{prod.}$]	770.7	671.9	1127.8	2857.0	600.6	1921.8	1803.0	2195.4	2750.2	4721.6
Annualized Inv. [$/GJ]	2.2	1.9	3.3	8.3	1.8	5.6	5.2	6.4	8.1	13.7
Maintenance [$/GJ]	2.7	2.6	3.3	8.2	2.2	4.6	5.1	5.9	6.9	13.2
Resource cost [$/GJ]	13.3	13.8	12.4	32.1	11.5	10.4	19.2	18.1	17.5	49.4
Electricity cost [$/GJ]	0	0	0	0	5.9	10.2	15.4	-	-	-
Prod. cost [$/GJ]	18.2	18.4	19	48.6	21.4	30.7	44.8	30.4	32.4	76.3
$/t$_{CO2,avoided}$	80.7	82	86.7	142	105	175	163	99	119	156
Costs variation: 5.5-19.5$/GJ$_{res}$, 41.7-8.4$/GJ$_e$										
Prod. cost [$/GJ]	12.5-31.5	12.5-32.2	13.6-31.4	29.3-61.4	13.9-33.6	21.7-42.2	26.5-54.2	22.7-48.6	24.9-49.9	46.6-96.1
$/t$_{CO2,avoided}$	36-183	36-189	45-182	75-187	46-198	106-263	82-204	14-296	38-306	72-212

List of Figures

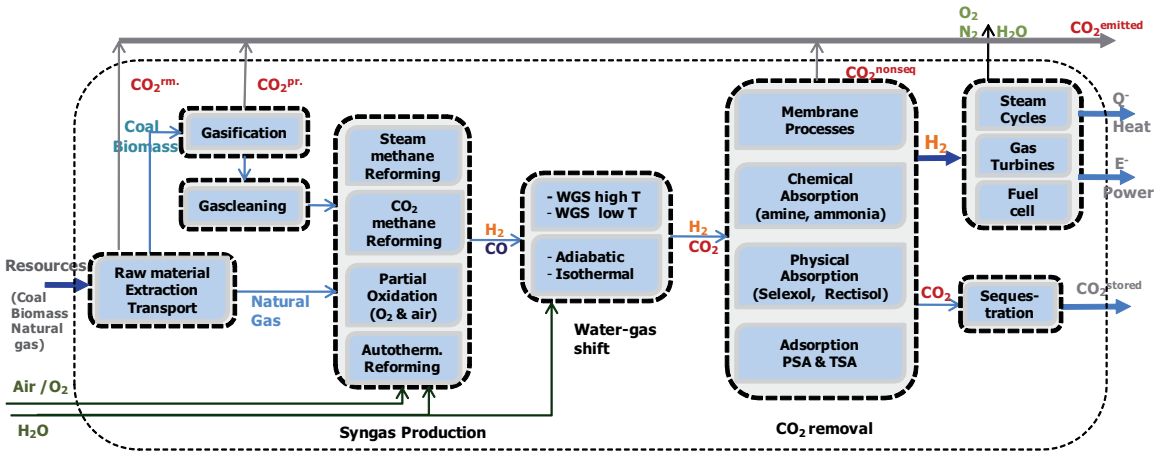

Figure 1: Process superstructure of pre-combustion process options.

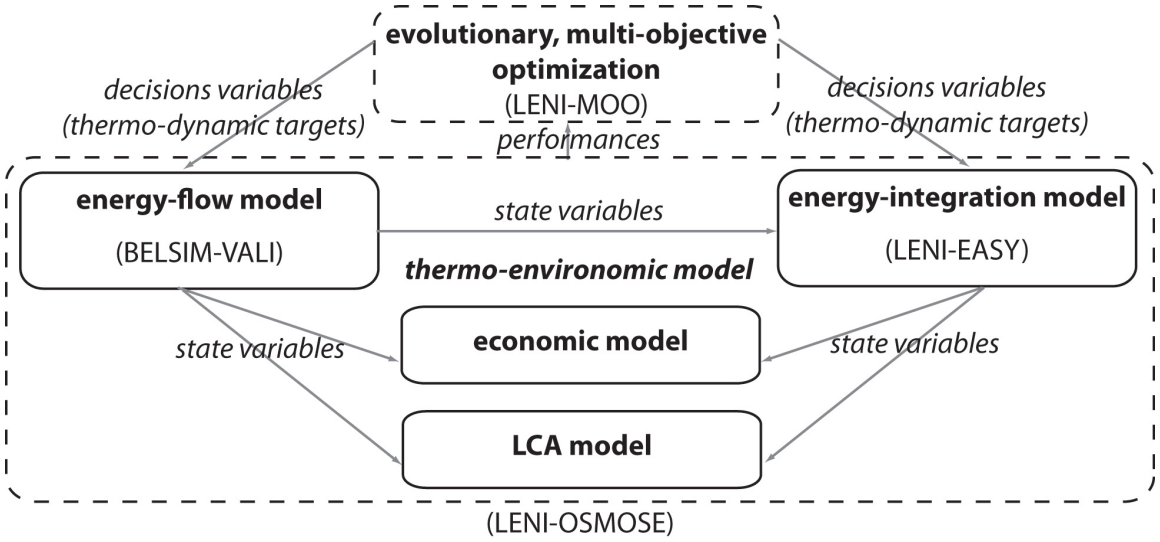

Figure 2: Design methodology: Thermo-economic optimization [13].

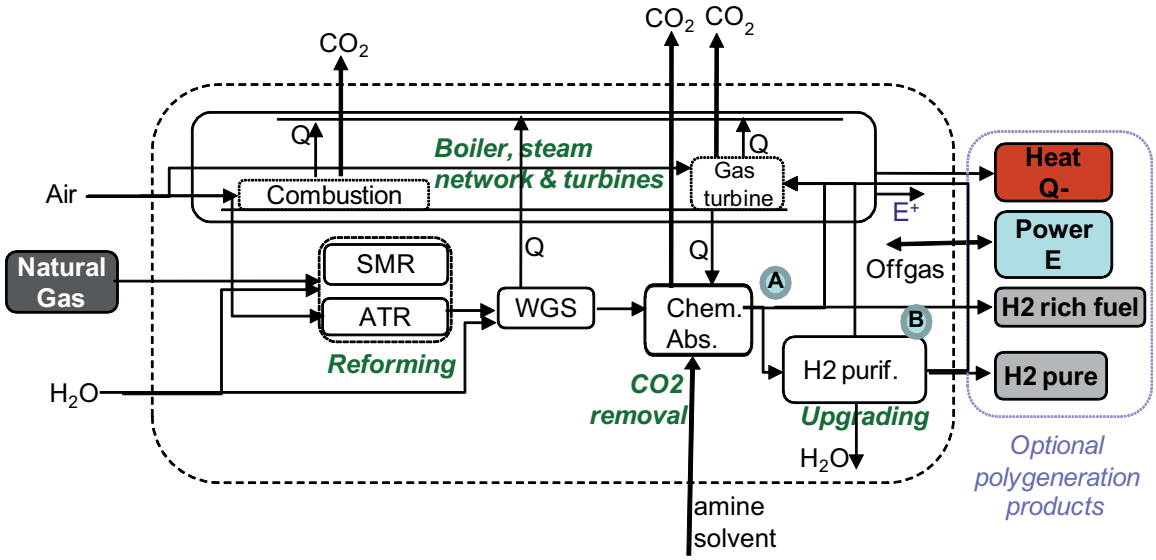

Figure 3: Process layout of the natural gas reforming processes. The products are defined by the decisions made at the cross points A and B.

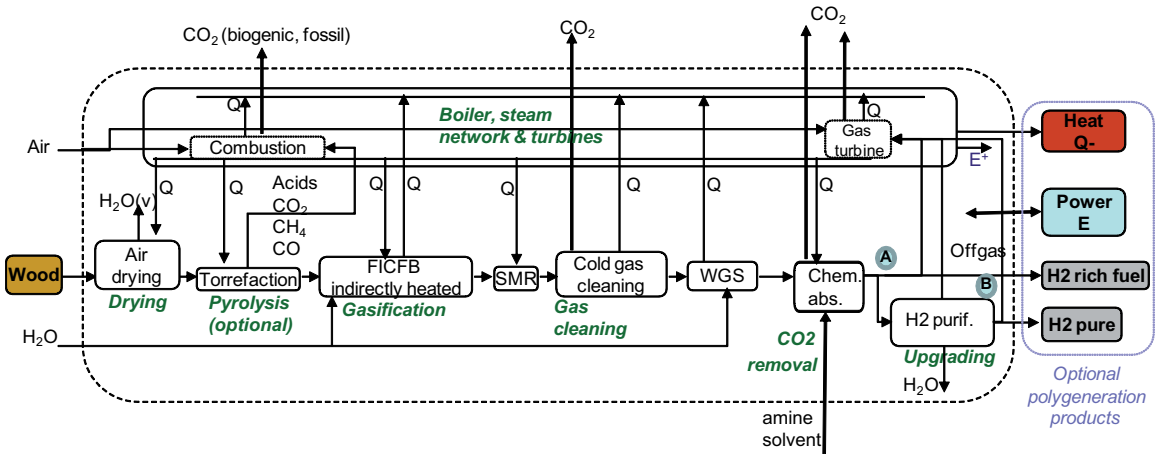

Figure 4: Process layout of the biomass conversion processes. The products are defined by the decisions made at the cross points A and B.

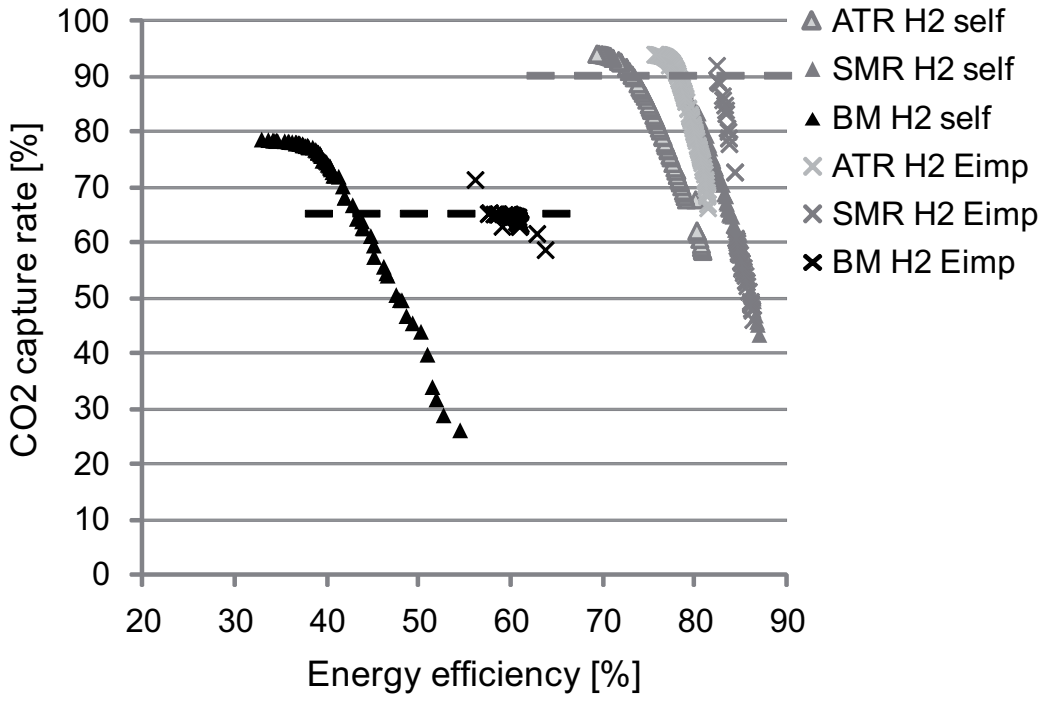

Figure 5: Pareto optimal frontier for H_2 production processes maximizing the energy efficiency and the CO_2 capture rate. Dashed lines represent the CO_2 capture level of configurations yielding a compromise with regard to both objectives.

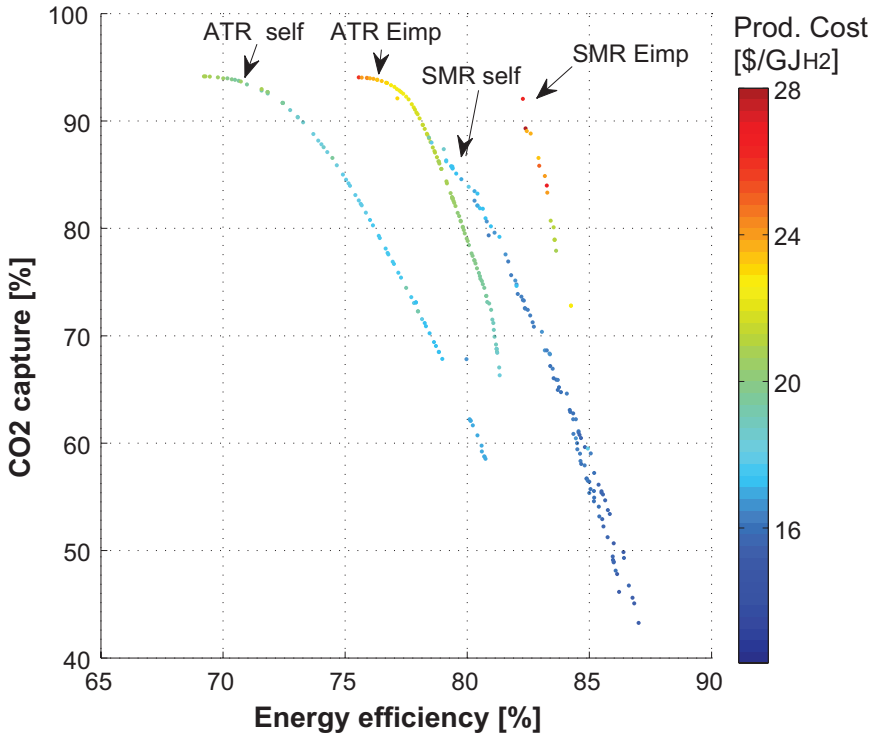

Figure 6: Multi-objective optimization results: trade-off between efficiency, CO_2 capture rate and production cost.

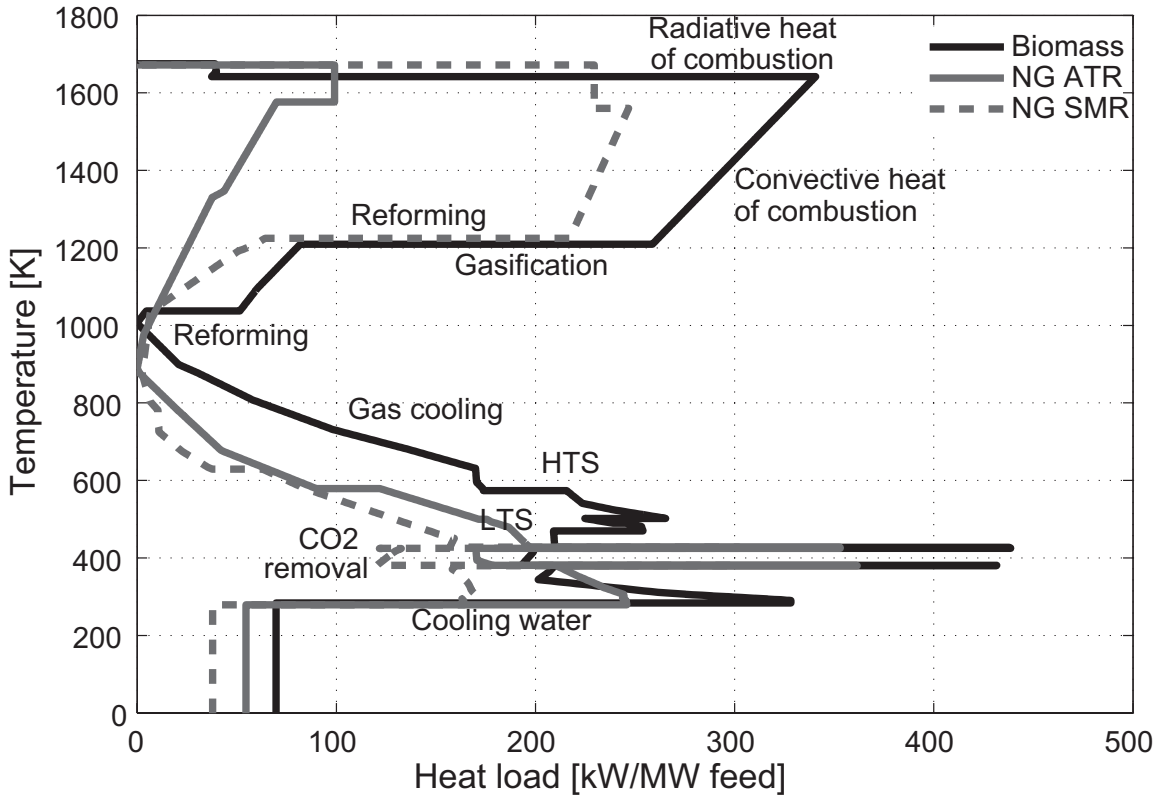

Figure 7: Integrated composite curves of self-sufficient H_2 production processes using different resources. The steam network integration is omitted on the figure for clarity.

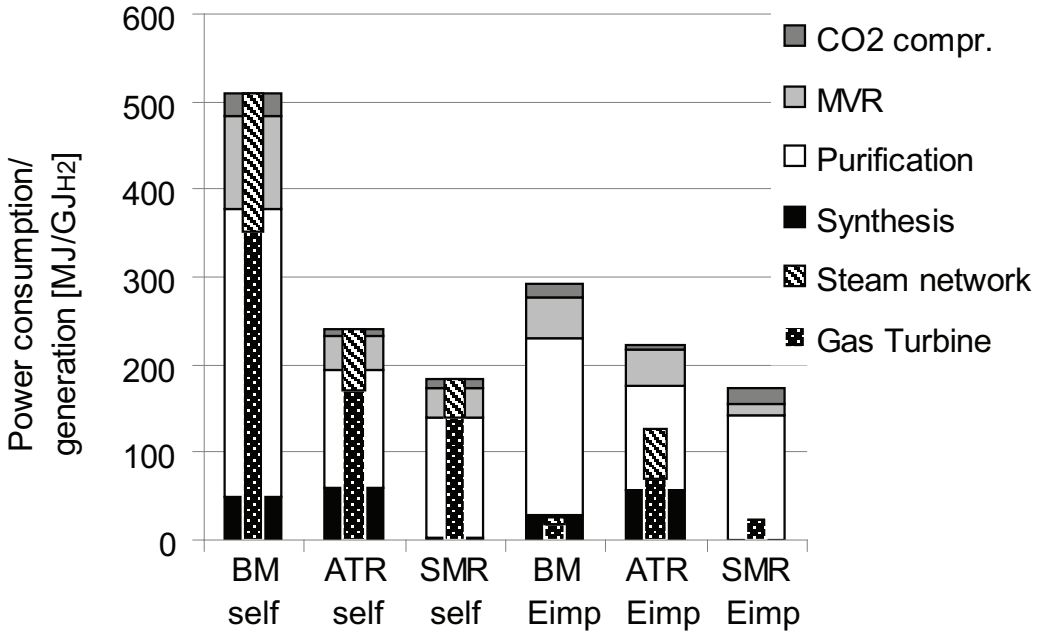

Figure 8: Power balance of different H_2 process configurations expressed in MJ per GJ of H_2 produced.

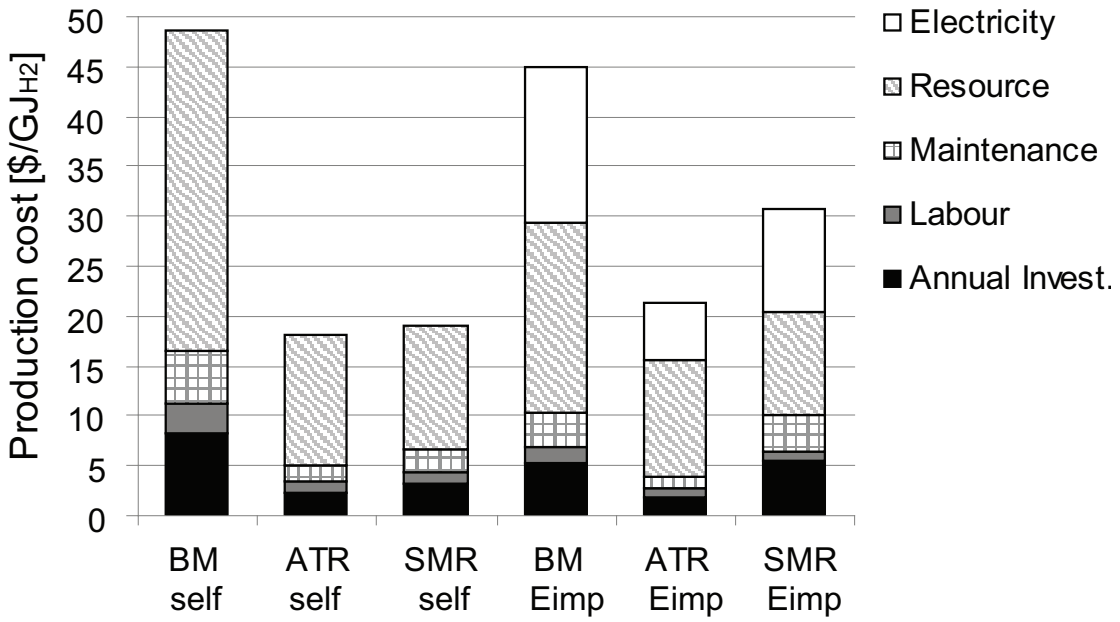

Figure 9: Production cost build-up [\$/GJ$_{H2}$] for different H_2 process configurations based on the base case economic assumptions reported in Table 4.

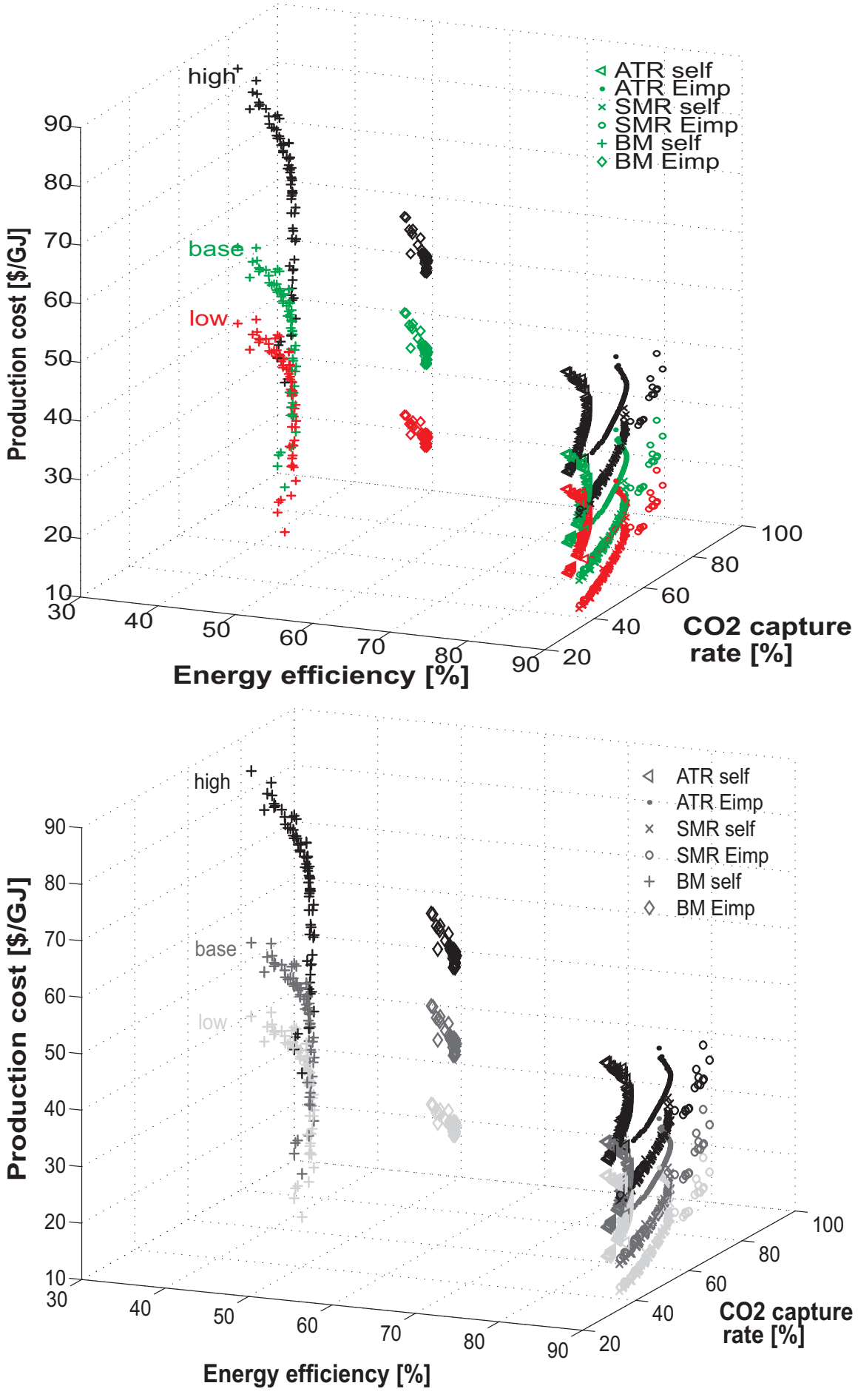

Figure 10: Production cost variation with regard to efficiency and CO_2 capture rate for the economic scenarios defined in Table 4.

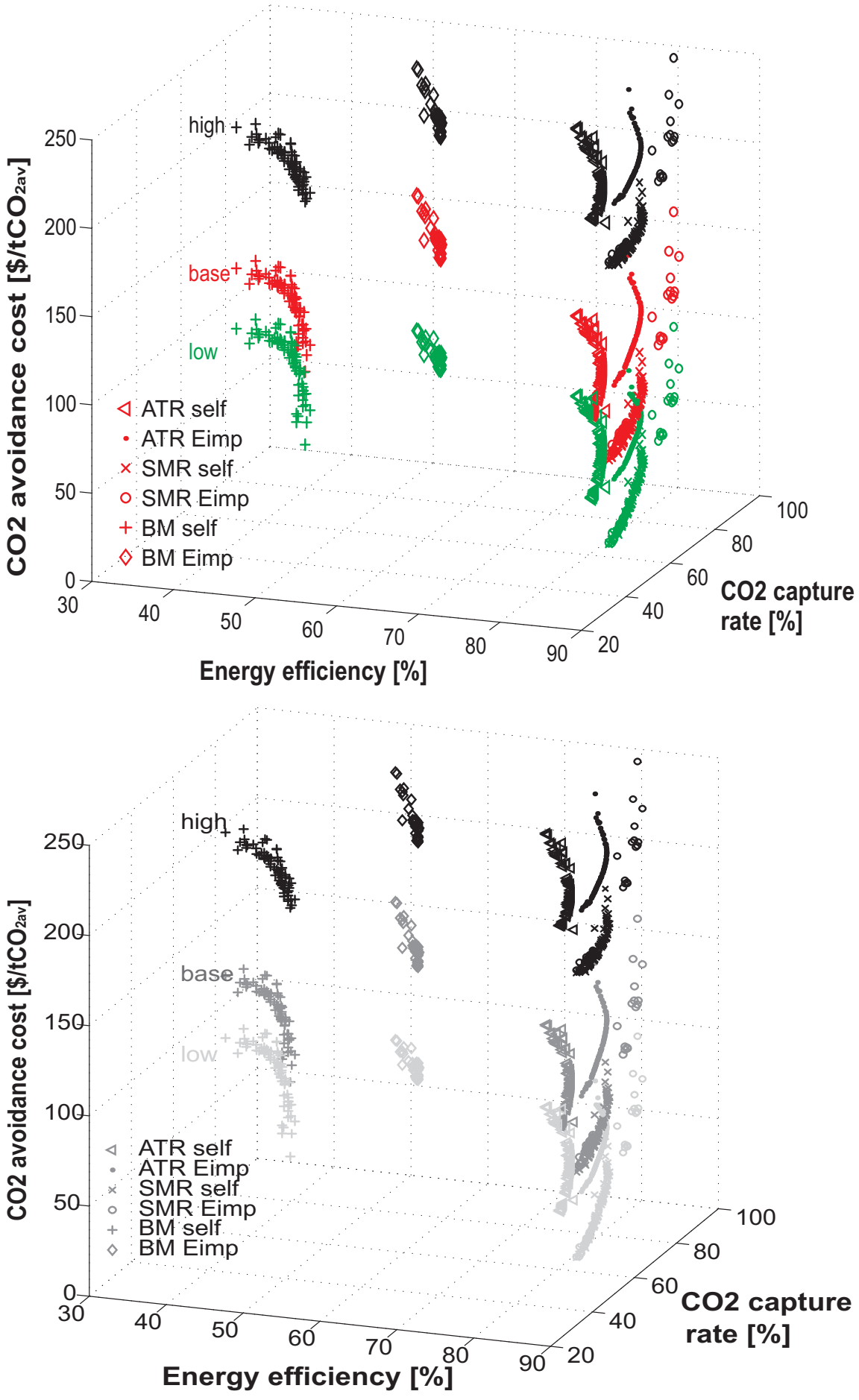

Figure 11: CO_2 avoidance cost with regard to efficiency and CO_2 capture rate. The variation range reflects the variation of the resource price on the production cost for the economic scenarios defined in Table 4. Reference H_2 process without CO_2 capture is taken from [23]: 7.8\$/GJ$_{H2}$ (with resource price 5\$/GJ$_{NG}$), 137kg$_{CO2}$/GJ$_{H2}$.

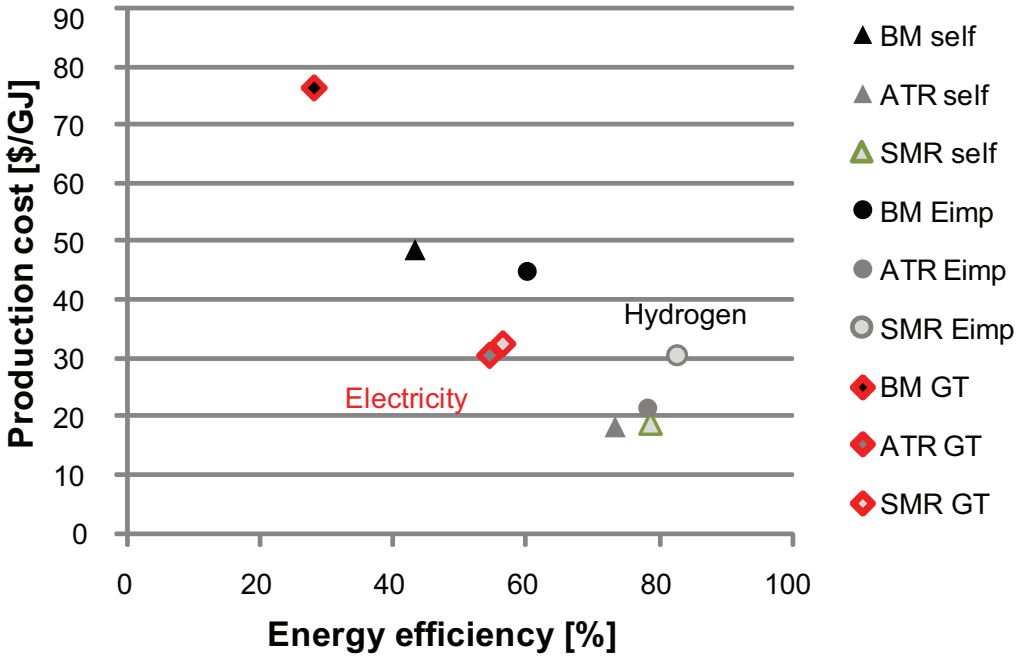

Figure 12: Product impact: Production cost (Table 4: base) versus energy efficiency of processes producing either H_2 or electricity (GT).